Mechanical Properties of Impact i-PP/CSM Rubber Blends

S. N. Maiti[a]; Rupak Das[a]

[a] Centre for Polymer Science and Engineering, Indian Institute of Technology, New Delhi, India

PLEASE SCROLL DOWN FOR ARTICLE

Taylor & Francis
Taylor & Francis Group

Mechanical Properties of Impact i-PP/CSM Rubber Blends

S. N. Maiti
Rupak Das
Centre for Polymer Science and Engineering,
Indian Institute of Technology, New Delhi, India

The impact strength and the tensile behavior of an impact grade of isotactic poly-propylene (impact i-pp)/chlorosulfonated polyethylene (CSM) rubber blends are studied at the CSM rubber concentrations 0 to 23.4 vol%. The impact strength, which increased with CSM rubber concentration, has been analyzed on the basis of the interphase adhesion and crazing mechanisms. Tensile modulus and strength decreased whereas breaking elongation increased with increase in CSM rubber content. Predictive models have been used to explain the tensile modulus and strength properties. Scanning electron microscopy has been employed to study the phase structure.

INTRODUCTION

Isotactic polypropylene (i-PP) is a very useful commercial polyolefin suitable for a wide variety of end uses [1–3]. The application range of the i-PP has been further widened by blending in it other polymers such as styrene-butadiene rubber [4], ethylene-propylene rubber [5–10], strene-ethylene-butylene-styrene rubber [11, 12], and so on. Currently, impact modified isotactic polypropylenes are manufactured by sequential copolymerization methods [3, 13–15]. Impact properties of such a copolymer may be further enhanced by an elastomer, and the resulting blend can be subsequently modified by use of various

467

fillers and reinforcements to achieve optimal property profiles at a reduced cost [3, 16].

In the present work an impact grade of i-PP, hereafter impact i-PP, was blended with varying concentrations of chlorosulfonated polyethylene (CSM) rubber. Mechanical properties, such as tensile and impact behavior, of the blends are evaluated on the basis of CSM concentrations. Morphology of the blend structure has been studied by scanning electron microscopy (SEM).

EXPERIMENTAL

Materials

A high impact reactor grade injection moldable isotactic polypropylene (impact i-PP) (B030MG) was obtained from Reliance Industries India Ltd. The polymer density was $0.9\,g/cc$ with an MFI value $3\,gm/10\,min$ and 18.5% rubber content [17]. Chlorosulfonated polyethylene (CSM) rubber, Hypalon 40, with density $1.18\,g/cc$ and chlorine content 35%, manufactured by DuPont, was used as the blending rubber [18]. The viscosity average molecular weight (M_v) of Hypalon 40 in toluene at $313\,K$ was 78,000 [19, 20]. Tribasic lead sulfate (density $7.1\,g/cc$) and lead strearate (density $7.23\,g/cc$) were obtained from Fine Chemicals India Ltd. and Pioneer Chemical Co. Ltd., respectively.

Blend Preparation

Blends of the impact i-PP and Hypalon 40 (together with 0.4 phr [based on rubber] of both lead sulfate and lead stearate heat stabilizers) at Hypalon contents 0–40 phr (0–23.4 vol%) were made by melt mixing the polymers in a Klockner-Windsor single screw extruder (Model $S \times 30$, $L/D = 20/1$) at 453–473 K using a screw speed of 20 rpm. Prior to blending the CSM rubber was cut into small pieces for better homogenization. The extruded strands were quenched in a water bath and granulated after drying in vacuum oven at 353 K for 2 h. The unblended impact i-PP was also subjected to identical extrusion process to ensure the same thermal history as the blends.

Preparation of Test Samples

Specimens for mechanical property determination were made by injection molding of the granules of the blend on a Windsor SP-1 screw-type machine using temperature 453, 463, and 473 K at the feed, compression, and die zones, respectively. The injection pressure and mold

locking pressures were 12 MPa and 1.9 Gpa whereas the mold temperature was 301 ± 2 K.

Measurement of Mechanical Properties

A Zwick Universal Tester (Model Z010) was used to measure tensile properties using dumb-bell shaped samples according to the ASTM D638 test procedure [21]. The gauge length used was 6 cm and a strain rate of 83.3% (i.e., cross-head speed 5 cm min^{-1}) was used. Izod impact strength of notched specimens were determined on a falling hammer-type impact tester (FIE instrument, Model IT-0.42) following the ASTM D 256 test method [21]. At least five samples were tested at each blend composition and the average value is reported. All tests were carried out at ambient temperature of 301 ± 2 K and at 65% RH.
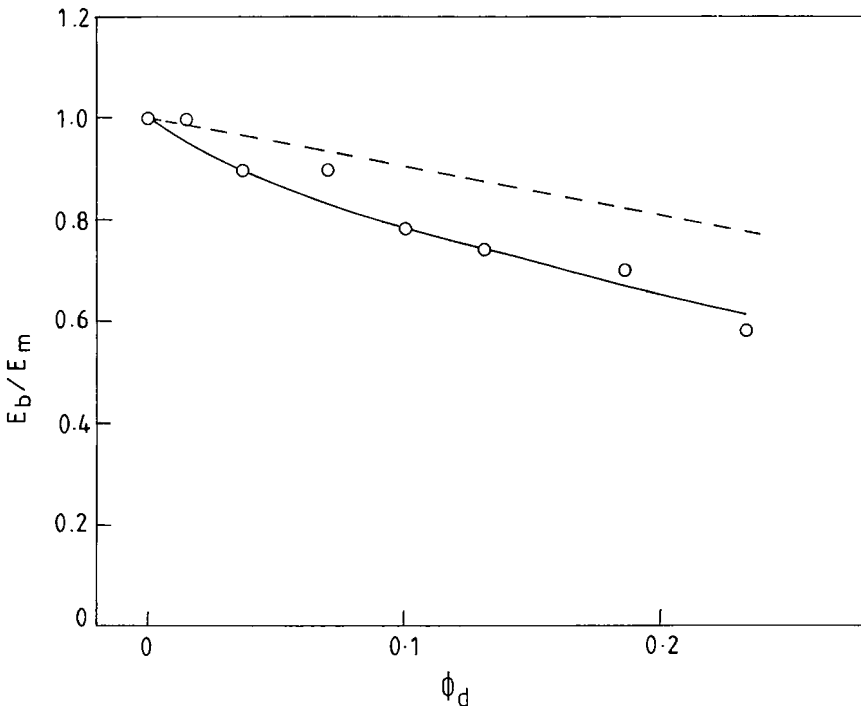
FIGURE 1 Plot of the relative tensile modulus (E_b/E_m) of (○) impact i-PP/CSM rubber blends and the predictive models according to the (−−−) "rule of mixtures" (Eq. 1), and the (—) "foam model" (Eq. 2), against ϕ_d.

Scanning Electron Microscopy (SEM) Studies

Cryogenically fractured surfaces of the dumb-bell specimens were scanned on a Cambridge stereoscan (Model 360) to examine the dispersion of the CSM rubber in the impact i-PP. Fractured surfaces were etched in toluene at 398 K for 12 h to remove the soluble rubber phase and then sputter-coated with silver prior to scanning.

RESULTS AND DISCUSSION

Tensile Properties

The tensile data were evaluated from the stress versus strain variations (not shown) and are shown in Figures 1–4 as the plots of the ratio of the property of the blends (subscript b) to that of the neat impact i-PP (subscript m) as functions of volume fraction of the
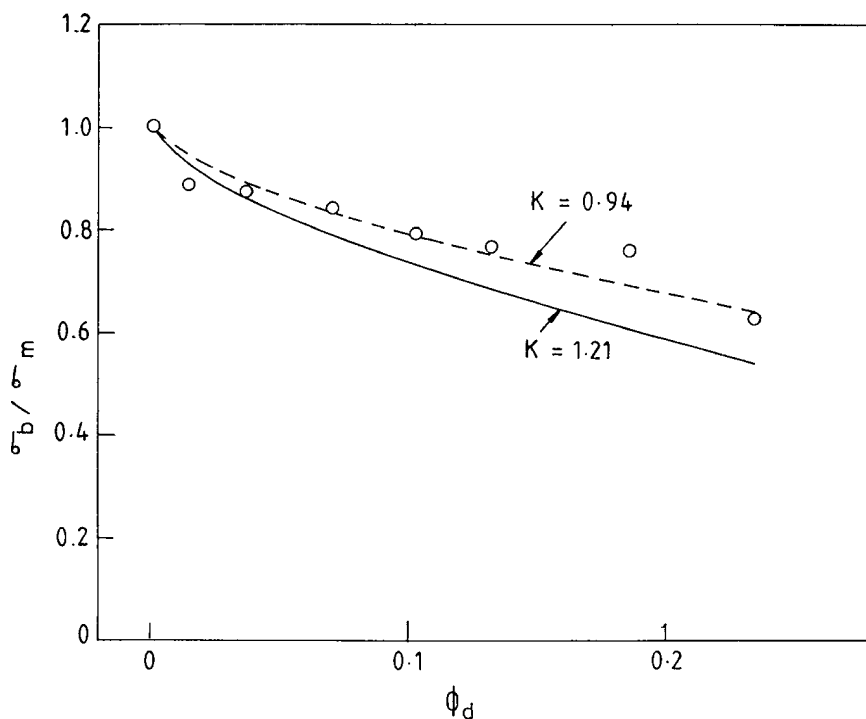
FIGURE 2 Variation of the relative tensile stress σ_b/σ_m of (○) impact i-PP/CSM rubber blends and the Nicolais–Narkis model (Eq. 3) with (– – –) K = 0.94 and (—) K = 1.21, vs. ϕ_d.
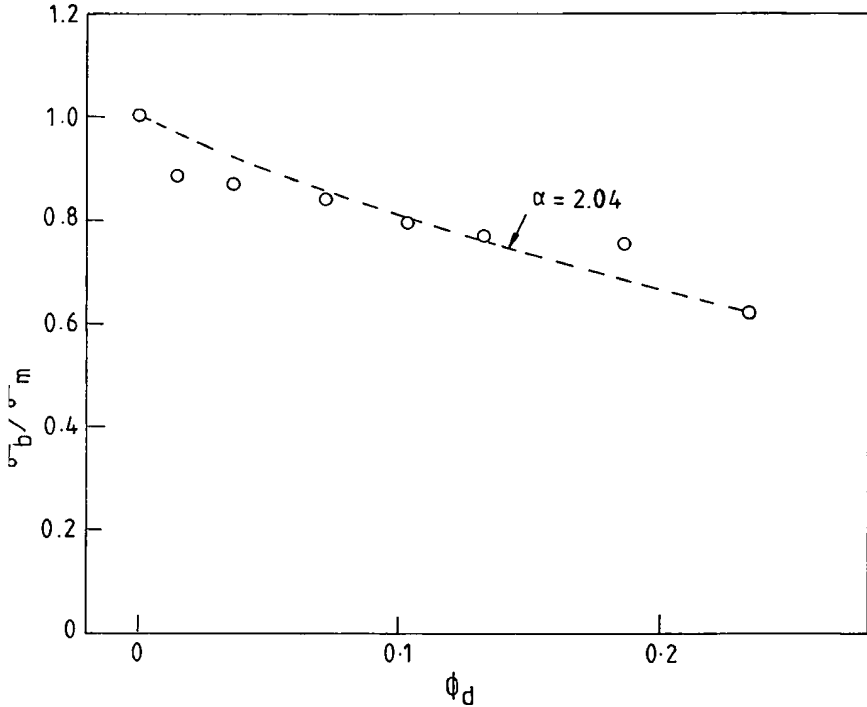
FIGURE 3 Plot of the relative tensile stress σ_b/σ_m of (○) impact i-PP/CSM rubber blends and the (−−−) porosity model with $\alpha = 2.04$ against ϕ_d.

dispersed phase (ϕ_d), that is, the blending polymer Hypalon 40 (CSM rubber).

Tensile Modulus

The plots of variations of the relative tensile moduli (E_b/E_m) of the impact i-PP/CSM rubber blends are presented in Figure 1 as functions of volume fraction, ϕ_d. The modulus showed a continuous decrease with increase in ϕ_d. The data were compared with the theoretical values according to the "rule of mixtures" as in composites [22], Eq. 1, as well as a "foam model" proposed by Cohen and Ishai [23], Eq. 2:

$$E_b/E_m = (E_d/E_m - 1)\phi_d + 1 \qquad (1)$$

$$E_b/E_m = (1 - \phi_d^{2/3}) \qquad (2)$$

In these calculations the moduli values of the impact i-PP (E_m) and the blends (E_b) were estimated from the initial slopes of the stress versus
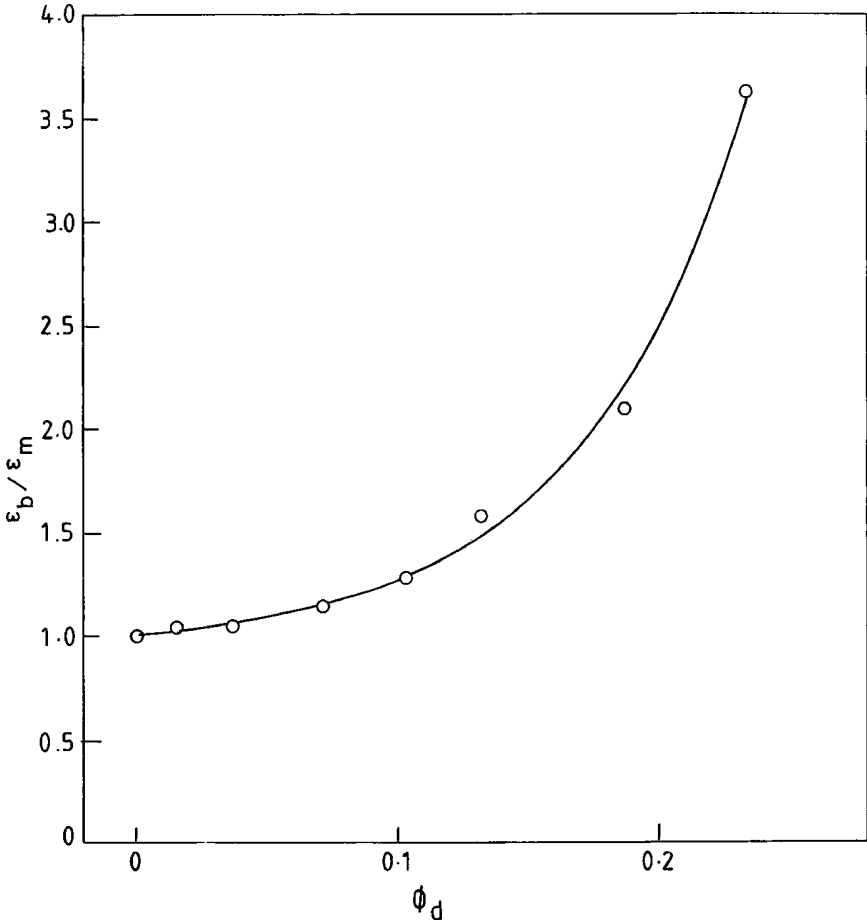
FIGURE 4 Dependence of the relative elongation at break $\in_b/\in_m$ of the impact i-PP/CSM rubber blends as functions of the ϕ_d.

strain curves whereas the modulus value of the CSM rubber (E_d) was taken at 300% strain [18]. In the foam model the rubber phase was considered as the noninteracting phase equivalent to a void or a pore so that the modulus of the rubber and the modular ratio of the rubber/matrix becomes zero. The "rule of mixture" curve showed higher values whereas the "foam model" exhibited reasonably good fit with the data, Figure 1. This indicates that the dispersed rubber phase decreases the stiffness of the impact I-PP, and the noninteracting rubber phase functions as pores or voids. This is, however, quite expected.

TABLE 1 X-Ray Crystallinity (%) of i-PP in Impact i-PP/CSM Rubber Blends

Blend composition (ϕ_d)	Weight fraction of i-PP	Normalized crystallinity (%)
0	0.82	68.9
0.07	0.74	66.8
0.13	0.68	65.3
0.18	0.63	61.9
0.23	0.58	53.1

The CSM rubber is a low modulus elastomer with a modulus $\sim 1/100$ of that of the impact i-PP matrix so that the plastic phase becomes significantly softened, which facilitates its deformability. An extent of decrease in crystallinity of i-PP in the presence of the rubber may also contribute to this softening effect [24] (Table 1). Plastic matrix softening by use of an elastomer increases its filler adoptability [16]. Other works also reported modulus decrease of polymer matrices upon elastomer incorporation [10, 25–26].

Tensile Strength

Figures 2 and 3 present variations in the relative tensile strength (ratio of tensile strength of impact i-PP/CSM rubber blend to that of the impact i-PP, (σ_b/σ_m) versus dispersed phase volume fraction, ϕ_d. Incorporation of the CSM rubber decreased the tensile strength of the impact i-PP and the data exhibited the decreasing trend with increase in the rubber concentration. This indicates weakening of the matrix polymer structure on account of the decrease in the effective matrix cross-sectional area due to the presence of the elastomer similar to other results [26–28]. Decrease in crystallinity of the impact i-PP component will also contribute to this decrease in tensile strength.

Some theoretical models were used to understand the weakness in the blend structure brought about by the elastomer phase. Similar theories, depicted by Eqs. 3 and 4, were used in other two-phase systems of polymer blends and composites, too, to analyze the structure [28–30]. The blend structure

$$\sigma_b/\sigma_m = (1 - K\phi_d^{2/3}) \tag{3}$$

$$\sigma_b/\sigma_m = \exp(-\alpha\phi_d) \tag{4}$$

was essentially no-adhesion type and is governed by either area fraction or volume fraction of the inclusion [30–32]. In Eq. 3 the area

fraction of the dispersed phase is assumed operative and the inter-phase interaction parameter K, also known as weightage factor, is a function of the blend structure [31–33]. The parameter K assumes a value of 1.1 for hexagonal packing of the inclusion in the plane of highest density. For spherical inclusions with poor adhesion K = 1.21 [32, 34], whereas K = 1 stands for strain considerations [35]. While K = 0 describes the unblended matrix polymer, values of K < 1.21 indicate better interphase adhesion; the lesser the value the better the adhesion [36, 37]. Eq. 4 describes the porosity model where the nonadhering minor phase is assumed to be in the form of pores/voids in metal, ceramic, or polymer matrices without any contribution to the mechanical properties of the two-phase systems [38, 39]. The defects in the structure are reflected in the value of the parameter α, the higher the value the higher the degree of weakness or stress concentration in the structure [32].

Table 2 exhibits the values of K and α estimated at each volume concentration of the minor phase CSM rubber by comparing the tensile strength data with the predictive models, Eqs. 3 and 4. The Nicolais–Narkis model, Eq. 3, shows that the stress concentration parameters were either less than or higher than unity depending on the value of ϕ_d implying significant weakness in the blend structure similar to other works [25, 28–29]. Significant weakness is also noted following the porosity model, Eq. 4, where the average value or α was ~2.04.

In Figures 2 and 3 the experimental tensile strength values are compared with the theoretical models, Eqs. 3 and 4, respectively.

TABLE 2 Values of Interphase Adhesion Parameter K (Eq. 3), and Stress Concentration Constant α (Eq. 4) in i-PP/CSM Rubber Blends

ϕ_d	K	α
0	—	—
0.02	0.19	8.17
0.04	1.16	3.74
0.07	0.95	2.50
0.10	0.94	2.24
0.13	0.89	1.98
0.18	0.75	1.50
0.23	0.98	1.99
Mean value	0.94	2.04

Due to data scatter, the mean value was estimated excluding some data points, e.g., for K at $\phi_d = 0.02$; for α at $\phi_d = 0.02$ and 0.04.

The data show a reasonably good fit with the Nicolais–Narkis model, Eq. 3, with a K value of 0.94 indicating a degree of interphase adhesion in the impact i-PP/CSM rubber blends. The adhesion may be due to the interaction of the rubbery polyethylene moiety with that of the EPR component of the impact i-PP [3]. However, the interphase of the blend generates quite significant weakness so that the body fails at large solid displacements similar to other two-phase systems [25, 28, 29, 40].

Good agreement is shown by the σ_b/σ_m data with the porosity model where the value of α is 2.04, Figure 3 and Table 1. A higher value of α indicates significant stress concentration in these blends as also observed in other reports [25, 28, 30, 40].

Breaking Elongation

Figure 4 presents the relative elongation at break data, $\in_b/\in_m$, as function of ϕ_d. The elongation of the impact i-PP increased in the presence of the CSM rubber. The data at first showed a marginal increase up to $\phi_d = 0.04$ whereas beyond this ϕ_d the increase was from $\sim$15% to 260%, depending on ϕ_d, compared to the impact i-PP. This implies that the impact i-PP is further softened by the CSM rubber facilitating molecular deformation of the plastic. The modulus data also indicated matrix softening by the elastomer CSM. Matrix softening also indicates toughening of the impact-PP, which will consume additional energy to break, as observed in other works as well [25, 41, 42].

Impact Behavior

The relative Izod impact strength (I_b/I_m) data of the blends are plotted against ϕ_d Figure 5. The value increases with the rubber content CSM, by $\sim$10–200% as the ϕ_d increased from 0.02 to 0.23, compared to that of the impact i-PP. Thus, the elastomer CSM substantially toughens the impact i-PP.

The increase in the impact strength of the impact i-PP in the presence of the CSM rubber may be attributed to the formation of ligaments with thickness less than a critical ligament thickness T_c [43]. This would promote shear-yielding, which in turn enhances the impact strength. The shear yielding in these blends may initiate at the interphase boundaries where high stress concentrations are generated, leading to local strain inhomogeneties observed earlier [41, 42]. Indication of generation of significant extent of stress concentration was obtained in the analysis of the tensile stress values in the previous section.
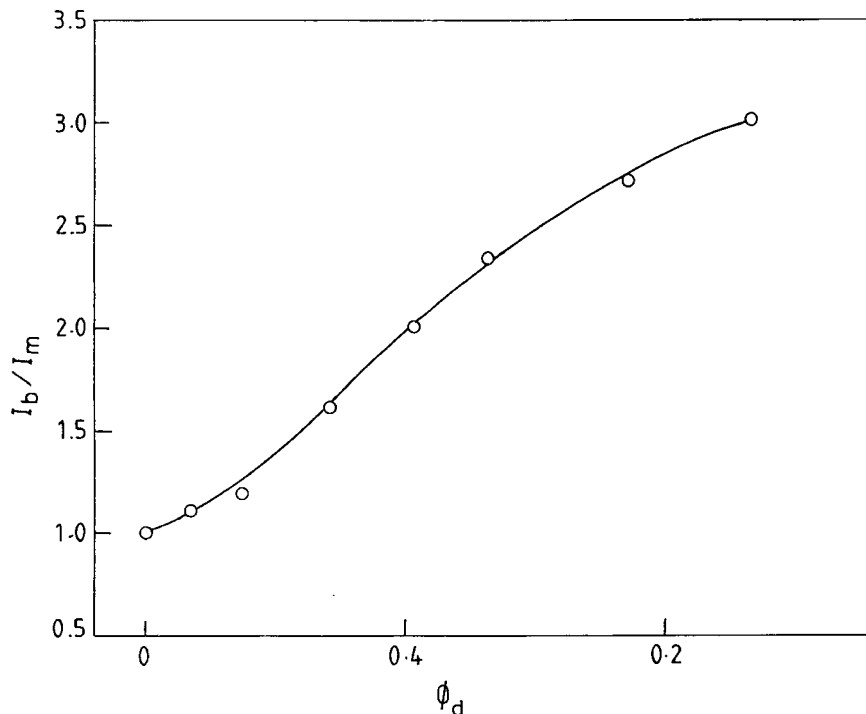
**FIGURE 5** Plot of the relative lzod impact strength I_b/I_m of the impact I-PP/CSM rubber blends vs. ϕ_d.

Fracture Surface Morphology

Figure 6a–d shows the SEM photomicrographs of the impact i-PP and impact i-PP/CSM rubber blends. In the impact i-PP the matrix consists of the i-PP whereas the reactor generated elastomer is dispersed as spherical granules some of which are etched completely, leaving cavities in the matrix (Figure 6a). A few of the granules are still adhering to the matrix. These may contain substantial amount, of the i-PP component. Incorporation of the blending rubber CSM up to $\phi_d = 0.07$ did not change the morphology to an appreciable extent, although a few ridges are observed indicating matrix softening (Figure 6b). However, on further increase in the CSM rubber content the shape of the dispersed phase deformed from spherical to elongated inclusions with significant enhancement in the size of the particles (Figures 6c and d). While the enhancement of dispersed phase size may be due to coalescence of rubber droplets at higher CSM rubber contents, the elongated
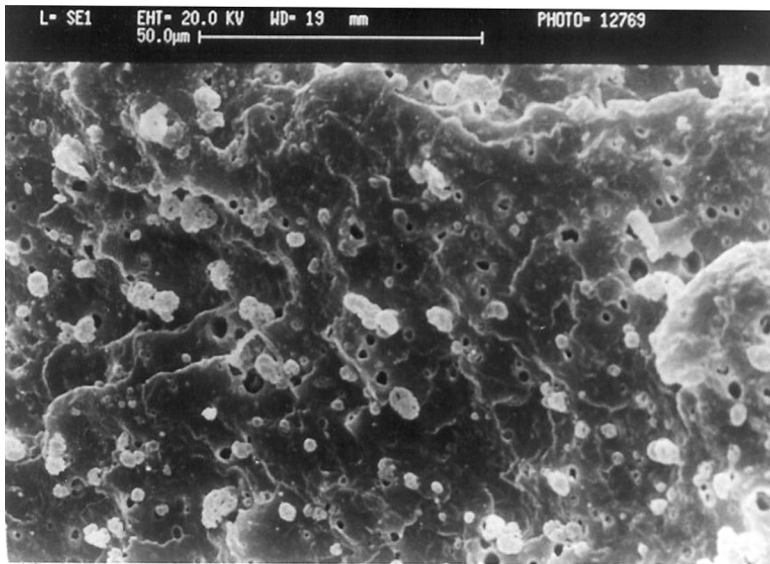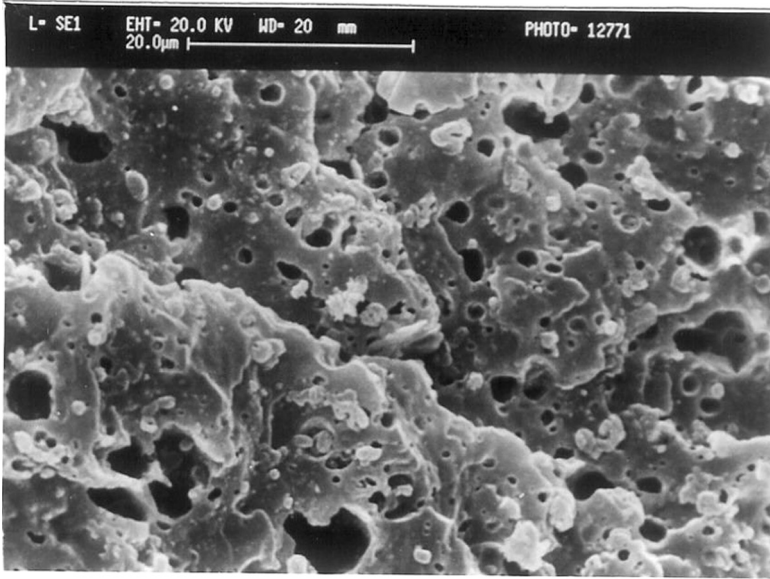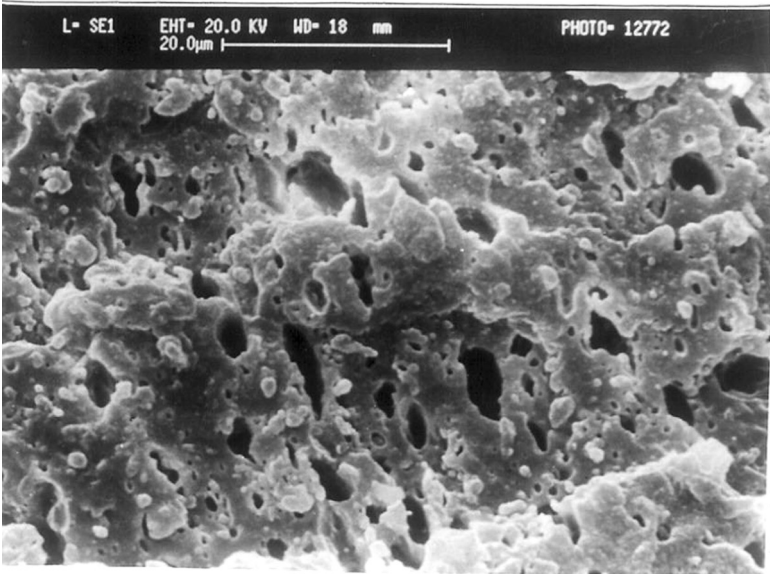
(a)
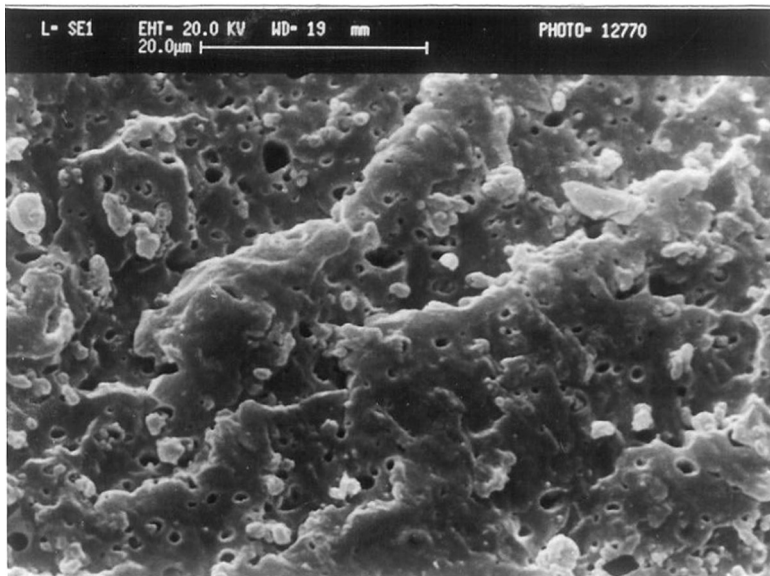
(b)

FIGURE 6 SEM photomicrographs of (a) impact i-PP and impact i-PP/CSM rubber blends at varying ϕ_d: (b) 0.07; (c) 0.13; (d) 0.23.

(c)

(d)

FIGURE 6 Continued.

shape arises from the elongational flow of the softer rubber component in the harder plastic phase during the injection molding of the samples.

The SEM micrographs were analyzed on a Leica Image Analyser using a software Leica Qwin Version 1 to evaluate the domain sizes of the rubbery phase [44, 45]:

$$d_n = \Sigma n_i d_i / \Sigma n_i$$
$$d_w = \Sigma n_i d_i^2 / \Sigma n_i d_i$$
$$d_v = \Sigma n_i d_i^3 / \Sigma n_i d_i^2$$

where n is the number of the droplets, d the diameter of the droplet, and the subscripts n, w, and v denote the average sizes based on number, weight, and volume of the droplets, respectively. Table 3 shows the variations of the domain sizes and izod impact strength values as functions of the CSM rubber content, ϕ_d. All types of domain sizes increased with ϕ_d. This increased domain size would contribute toward decreasing the tensile modulus and strength and increasing the elongation and impact strength of the blends [44].

The increase in the impact strength of the impact i-PP/CSM rubber blends with increasing CSM rubber content and sequential increased domain size of the minor phase (Table 3), can be explained on the basis of craze initiation and cavitation processes. Craze initiation theory predicts that craze occurs around a rubber particle when it is stressed both in a direction perpendicular to the applied stress as well as in the plane of the craze perpendicular to the applied stress [46]. If the rubber particle is too small then they are completely embedded in the craze. Although small particles of rubber are more effective in toughening than the larger ones, very small particles might not cavitate at all.

The increase in impact strength at low concentrations of the CSM rubber may be due to the local microplastic deformation arising from

TABLE 3 Values of Domain Sizes and Impact Strength of Impact-PP/CSM Rubber Blends

CSM content Phr (ϕ_d)	d_n (µm)	d_w (µm)	d_v (µm)	Impact strength (J/m)
0 (0)	—	—	—	64
10 (0.07)	1.17	1.35	1.54	103
20 (0.13)	2.21	3.05	3.81	121
40 (0.23)	3.35	3.58	3.79	193

the microscopic cavities around the poorly bonded CSM rubber droplets [47]. At CSM rubber contents of 10 and 20 phr ($\phi_d = 0.07$ and 0.13) the number average rubber domain size was $1.17 \mu m$ and $2.21 \mu m$, which may be a degree less than the critical size (2.83–3.30 μm) for impact toughening so that crazing may be restricted. At 40 phr CSM concentration ($\phi_d = 0.23$) the domain size of droplets increased to 3.35 μm, which facilitated crazing of rubber particles resulting in a much enhanced impact strength of 193 J/m.

CONCLUSIONS

Incorporation of CSM rubber further enhances the Izod impact strength of an impact i-PP. Up to the rubber concentrations of 0.13 vol fraction the value doubled whereas at 0.23 vol fraction rubber the impact strength tripled. The increase in the impact strength depended on the domain size of the dispersed phase. Up to 0.13 vol fraction rubber the impact toughening was ascribed to a microplastic deformation arising out of small cavities formed at the interphase whereas at higher rubber content the domain size increased facilitating crazing, which in turn led to a significant increase in impact strength.

The tensile modulus and strength of impact i-PP decreased whereas elongation at break increased on addition of the CSM rubber. The rubber gives rise to matrix softening. Analysis of the tensile properties on the basis of the blend composition in terms of various models provides information about the interphase adhesion and the formation of stress concentration points in the matrix polymer.

Scanning electron microscopy studies indicate a two-phase structure with fine globular rubber dispersal in the impact i-PP. At low CSM rubber content the two phase morphology is maintained and the globular size does not show appreciable change. At higher CSM rubber content the shape of the dispersed phase changes from spherical to elongated with enhanced particle size. This increased domain size of the dispersed phase enhances the impact strength and softens the matrix.

REFERENCES

[1] Brydson, J. A. (1999). *Plastics Materials*, 7th ed., Butterworth–Heinemann, Oxford, Ch. 11.
[2] Mark, H. F., Bikales, N. M., Overberger, C. G., Menges, G., and Kroschwitz, J. I. Eds. (1988). *Encyclo. Polym. Sci. Eng.*, V.13, John Wiley and Sons, New York, p. 464.
[3] Moore, E. P. Jr., Ed. (1996). *Polypropylene Handbook*, Hanser, New York.

[4] Bohn, G. G. A., Hamed, G. R., and Yescilius, L. E. Ger. Offen, 2,825,697 (1978).

[5] Paul, D. R. and Newman, S. (1978). *Polymer Blends*, Vol. 2. Academic, New York.

[6] Stehling, F. C., Huff, T., Speed, C. S., and Wissler, G. *J. Appl. Polym. Sci.* **26**, 2693 (1981).

[7] Karger-Kocsis, J. and Kiss, L. *Polym. Eng. Sci.* **27**, 254 (1987).

[8] Pukanszky, B., Tudos, F., Kallo, A., and Bodor, G. *Polymer* **30**, 1399 (1989).

[9] Kolarik, J., Agarwal, G. L., Krulis, Z., and Kovar, J. *Polym. Compos.* **7**, 463 (1986).

[10] Jancar, J., Di Anselmo, A., Di Benedetto, A. T., and Kucera, J. *Polymer* **34**, 1684 (1993).

[11] Gupta, A. K. and Purwar, S. N. *J. Appl. Polym. Sci.* **29**, 1079 (1984).

[12] Gupta, A. K. and Purwar, S. N. *J. Appl. Polym. Sci.* **31**, 535 (1986).

[13] Galli, G., Simonazzi, T., and Barbe, P. C. (October), Proc. of 6 Italian Symposium on Macromolecular Science, Pisa, Italy (1983).

[14] Cecchin, G. *Macromol. Symp.* **78**, 213 (1994).

[15] Brintzinger, H. H. (1988). In *Transition Metals and Organometallics as Catalysts for Olefin Polymerization*. W. Kaminsky and H. Sinn, Eds., Springer-Verlag, Berlin, p. 249.

[16] Katz, H. S. and Milewski, J. V. (1987). *Handbook of Fillers and Reinforcements of Plastics*, Van Nostrand Reinhold, New York.

[17] Product Bulletin, Reliance Industries Ltd. (2000). Repol® Homopolymers, Mumbai.

[18] Product literature, Du Pont Ltd. (2000). Chlorosulfonated Polymers (CSM), New York.

[19] Gowarikar, V. R., Viswanathan, N. V., and Sreedhar, J. 2003, Polymer Science, New Age International (P) Ltd., New Delhi.

[20] Brandrup, J., Immergut, E. H., and Grulke, E. A. (1981). *Polymer Handbook*, John Wiley & Sons, New York.

[21] *Annual Book of ASTM Standards* (1976). Philadelphlia, Part 37.

[22] Agarwal, B. D. and Broutman, L. J., Eds. (1990). *Analysis and Performance of Fiber Composites*, John Wiley & Sons, New York.

[23] Cohen, L. J. and Ishai, O. *J. Compos. Mater.* **1**, 399 (1963).

[24] Das, R. (2000). M. Tech. Dissertation, Indian Institute of Technology, New Delhi.

[25] Maiti, S. N., Barman, N., and Gupta, A. K. Intern. J. Polym. Mater. **54**, 2005. This issue.

[26] Pukanszky, B., Tudos, F., Kallo, A., and Bodor, G. *Polymer* **30**, 1407 (1989).

[27] Chiang, W.-Y., Yang, W.-D., and Pukanszky, B. *Polym. Eng. Sci.* **32**, 641 (1992).

[28] Gupta, A. K. and Purwar, S. N. *J. Appl. Polym. Sci.* **30**, 1799 (1985).

[29] Gupta, A. K. and Purwar, S. N. *J. Appl. Polym. Sci.* **29**, 3513 (1984).

[30] Maiti, S. N. and Sharma, K. K. *J. Mater. Sci.* **27**, 4605 (1992).

[31] Piggot, M. R. and Leidner, J. *J. Appl. Polym. Sci.* **18**, 1619 (1974).

[32] Kunori, T. and Geil, P. H. *J. Macromol. Sci. Phys.* B. **18**, 135 (1980).

[33] Ramsteiner, F. and Theyson, R. *Composites* **15**, 121 (1984).

[34] Nicolais, L. and Nicodemo, L. *Int. J. Polym. Mater.* **4**, 229 (1974).

[35] Nielsen, L. E. *J. Appl. Polym. Sci.* **10**, 97 (1966).

[36] Nicodemo, L. and Nicolais, L. *Mater. Sci. Lett.* **2**, 201 (1983).

[37] Maiti, S. N. and Subbarao, R. *Int. J. Polym. Mater.* **15**, 1 (1991).

[38] Passmore, E. M., Spriggs, R. M., and Vasilos, T. J. *J. Amer. Ceram. Soc.* **48**, 1 (1965).

[39] Nielsen, L. E. *J. Compos. Mater.* **1**, 100 (1967).

[40] Mitsuishi, K., Kodama, S., and Kawasaki, H. *Polym. Eng. Sci.* **25**, 1069 (1995).

[41] Bucknall, C. B. (1977). *Toughened Plastics*, Applied Science, London.

[42] Dwyer, S. M., Boutni, O. M., and Shu, C. (1996). In *Polypropylene Handbook*. E. P. Moore, Jr., Ed., Hanser, New York.
[43] Wang, Y. and Jiang, S. *J. Appl. Polym. Sci.* **60**, 1779 (1996).
[44] Bhattacharya, A. R. (2000). Ph. D. Thesis, IIT Delhi, New Delhi.
[45] Image Processing and Analysis System, Leica Qwin User Guide, Cambridge (1996).
[46] Brydson, J. A. (1999). *Plastics Materials*, 7th ed., Butterworth–Heinemann, Oxford, Ch. 3.
[47] Silverstein, R. M., Bassler, G. C., and Morrill, T. C. (1981). *Spectometric Identification of Organic Compounds*, 4th ed., John Wiley & Sons, New York, p. 45.